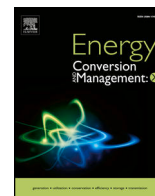# Journal Pre-proofs

Co-combustion of oil palm trunk biocoal / sub-bituminous coal fuel blends

Nadly Aizat Nudri, Wan Azlina Wan Abdul Karim Ghani, Robert Thomas Bachmann, B.T. Hang Tuah Baharudin, Denny Ng Kok Sum, Mohamad Syazarudin Md Said

Please cite this article as: N. Aizat Nudri, W. Azlina Wan Abdul Karim Ghani, R. Thomas Bachmann, B.T. Hang Tuah Baharudin, D. Ng Kok Sum, M. Syazarudin Md Said, Co-combustion of oil palm trunk biocoal / sub-bituminous coal fuel blends, *Energy Conversion and Management: X* (2020), doi: https://doi.org/10.1016/j.ecmx.2020.100072

This is a PDF file of an article that has undergone enhancements after acceptance, such as the addition of a cover page and metadata, and formatting for readability, but it is not yet the definitive version of record. This version will undergo additional copyediting, typesetting and review before it is published in its final form, but we are providing this version to give early visibility of the article. Please note that, during the production process, errors may be discovered which could affect the content, and all legal disclaimers that apply to the journal pertain.

Title

Co-combustion of oil palm trunk biocoal / sub-bituminous coal fuel blends

Authors

Nadly Aizat Nudri [a], Wan Azlina Wan Abdul Karim Ghani [a,b,*], Robert Thomas Bachmann [c], B.T. Hang Tuah Baharudin [d], Denny Ng Kok Sum [e] and Mohamad Syazarudin Md Said [a]

[a] Sustainable Process Engineering Research Centre (SPERC), Department of Chemical and Environmental Engineering, Faculty of Engineering, Universiti Putra Malaysia, 43400 Serdang, Selangor Darul Ehsan, Malaysia

[b] Institute of Plantation Studies, Universiti Putra Malaysia, 43400 Serdang, Selangor Darul Ehsan, Malaysia

[c] Section of Environmental Engineering Technology, Universiti Kuala Lumpur-Malaysian Institute of Chemical and Bioengineering Technology (UniKL-MICET), 78000 Alor Gajah, Melaka

[d] Department of Mechanical Engineering, Faculty of Engineering, Universiti Putra Malaysia, 43400 Serdang, Selangor Darul Ehsan, Malaysia

[e] School of Engineering and Physical Sciences, Heriot-Watt University Malaysia, No 1 Jalan Venna P5/2, Precinct 5, 62200 Putrajaya, Malaysia

*Corresponding author:
Email: wanazlina@upm.edu.my
Phone number: +603 9769 6287; Fax: +603 8656 7120

Abstract

Biomass is a promising alternative for the reduction of global dependency on fossil fuels. However, there are some issues with the direct application of raw biomass such as high moisture content, low heating value, and poor grindability. To alleviate the problems, biomass-derived biocoal is introduced and utilised as fuel in power plants. Oil palm trunk biocoal (OPTC) is produced from pyrolysis of oil palm trunk biomass (OPTB) in a top-lit, updraft reactor at a constant air flowrate of 4.63 L/min and maximum temperature of 550 °C. OPTC is co-combusted at temperatures between 600 to 900 °C with sub-bituminous coal (SBC). Pollutant emission and ash production of combustion of fuel blends containing 20% and 50% biocoal are analysed and compared with pure SBC, OPTB and OPTC. NOx and SO_2 emission profiles from all tested fuel blends are well below the limits imposed under Environmental Quality (Clean Air) Regulation 2014 of 296 and 190 ppm respectively. Response surface methodology (RSM) analysis indicates that the operation of combustion is optimised with 92.16% efficiency at 774 °C and air flowrate of 16.6 SCFH to emit 16.38% CO_2, and the findings are validated against experimental results. The optimised combustion process produces ash with 67.9% silicon compounds.

Keywords: biocoal; oil palm trunk; co-combustion; pyrolysis; optimisation

1.0 Introduction

Alternative energy resources are gaining significant attention due to the concerns on global climate change. The growth of the global economy and world population is forecasted to increase energy demand, hence increasing the greenhouse gas (GHG) emission[1], [2]. The large consumption of fossil fuels results in the emission of GHG that is responsible for environmental pollution, acid rain and global warming. Among fossil fuels, the carbon emission from coal combustion is the highest (43%) compared to oil (37%) and gas (20%) [3]. The use of renewable resources such as solar energy, wind power and biofuels has been promoted to reduce CO_2 emission. China has targeted to reduce CO_2 emission in 2030 by committing to increase the share of non-fossil fuels in primary energy consumption up to 20% [4]. Relatively, Malaysia is committed to achieve 50% of renewable energy in the energy mix by 2050 by utilising biomass as the energy resource in the power plant [5].

Due to the high productivity of the palm oil industry in Malaysia, oil palm derived biomass can be obtained in a vast amount. Oil palm derived biomass can be sourced from plantations and processing mills. From the plantation, the biomass is mostly present in the form of oil palm frond (OPF) and oil palm trunk (OPT) [6]. Currently, the annual production of oil palm trunk is 74.5 tonne per hectare [7]. Some portions of OPT are used to produce fibreboards, plywood, and furniture. However, only the outer parts of OPT is reusable since its poor mechanical structure is not desirable for furniture manufacturing [8]. The disposal of unwanted OPT is commonly done by open burning which causes a serious air pollution issue. Few studies were conducted on possible conversion into biofuel as OPT biomass is rich in sugar [9, 10]. Tareen, Sultan *et al.* [11] produced ethanol from enzymatic hydrolysis and fermentation of OPT.

Thermochemical route is a viable option for OPT biomass conversion into energy. The potential benefits of co-firing or co-combustion of sub-bituminous coal/oil palm biomass fuel blends have been discussed in [12]. In oil palm mills, OPT can be used directly as a solid fuel in the steam boilers for electricity production using steam turbines. However, direct OPT biomass utilisation incurs a high cost for fuel production and suffers from inefficient energy conversion due to the high moisture content, low energy density and low grindability nature of OPT biomass. To alleviate the problems, OPT biocoal is introduced as a feedstock for energy production. Biocoal is more preferable compared to raw biomass due to its desirable properties of low moisture content, high calorific value, lower density for storage and durability for long term storage. Nudri, Bachmann *et al.* [13] and Sakulkit, Palamanit *et al.* [14] used pyrolysis technique to produce biochar while Kamal Baharin, Koesoemadinata *et al.* [15] utilised hydraulic press machine and electric furnace to produce biochar. The discussion on improvement in biofuel characteristics brought by pyrolysis of oil palm trunk biomass is available in [13]. Nevertheless, none of these studies [13],[14],[15] conducted a combustion study of the OPTC to further evaluate its characteristics as a potential solid biofuel.

In this study, biocoal is produced from pyrolysis of oil palm trunk biomass. Gas emission and char production from co-combustion of oil palm trunk biocoal with sub-bituminous coal are investigated. The optimal conditions for co-combustion of oil palm trunk / sub-bituminous coal fuel blends are determined from response surface methodology and the findings are validated against experimental data. Statistical analyses are conducted to investigate the dominance of process temperature and air flowrate on combustion efficiency and carbon dioxide emission. The relationships connecting air flow rate and process temperature with combustion efficiency and

carbon dioxide emission are determined from regression analysis and presented in second-order polynomial.

2.0 Materials and method

2.1 Material preparation

The oil palm trunk biomass (OPTB) was procured from an oil palm plantation in Semenyih in chipped form. The OPTB was sun-dried, shredded and sieved into 1 to 3.35 mm particles. The shredded OPTB particles were pyrolysed into biochar (or biocoal) (OPTC) in a top lift updraft, autothermal-heated furnace using a method adopted from Nsamba, Hale *et al.* [16]. Sub-bituminous coal (SBC) was obtained from Tenaga Nasional Berhad (TNB) Janamanjung power plant in Manjung, Perak. Proximate and ultimate analyses of both oil palm trunk biomass and biocoal as reported in [13] are shown in **Table 1**.

Table 1. Proximate and ultimate analyses of OPT, OPTC and coals [13].

	Elemental Analysis [a](daf)				Proximate Analysis [b](db)		
	C	H	N	O*	[c]VM	[d]FC	Ash
[e] Raw OPT biomass	46.1	5.77	2.44	45.8	81.7	12.1	6.22
Raw OPT biomass (this study)	50.1	7.59	1.04	41.2	77.1	4.29	18.6
[e] OPT Biocoal	58.7	2.46	3.41	35.5	31.4	42.5	26.1
OPT Biocoal (this study)	67.9	3.49	1.43	26.7	41.3	30.9	27.8
Sub-bituminous coal (this study)	77.6	7.22	0.93	13.7	39.4	51.8	15.5
[f] Lignite coal	66.1	4.70	0.73	30.1	49.2	47.0	3.83
[g] Bituminous coal	83.5	4.95	1.90	8.01	34.6	60.3	5.10

*Oxygen calculated by difference, [a]dry ash free basis, [b]dry basis, [c]Volatile matter, [d]Fixed carbon, e[17], f[18], g[19]

2.2 Experimental setup and procedures

The combustion process was conducted in a bench-scale system that consists of a heat resistant stainless-steel reactor, condenser, gas clean-up unit and gas sampling unit. The schematic diagram of the rig arrangement is shown in **Fig. 1**. Two individually controlled electric furnaces are used to cover the reactor for heating purposes and preventing heat loss to the atmosphere during operation. Two thermocouples (K-type) were installed, one in the middle of the reactor and one on top of the reactor (freeboard) to monitor the temperature during experimental operation. During the experiment, limited air was supplied by an external compressor and was introduced into the reactor from the base of the bed through a nozzle. The gas produced from feedstock combustion flowed into the gas condenser followed by the gas clean up section for dust particle filtration. The clean gas was then collected using gas sampling bag and sent for offline GC analysis. The reactor was cooled down for ash collection which was manually removed from the bottom lid of the reactor for further analyses.
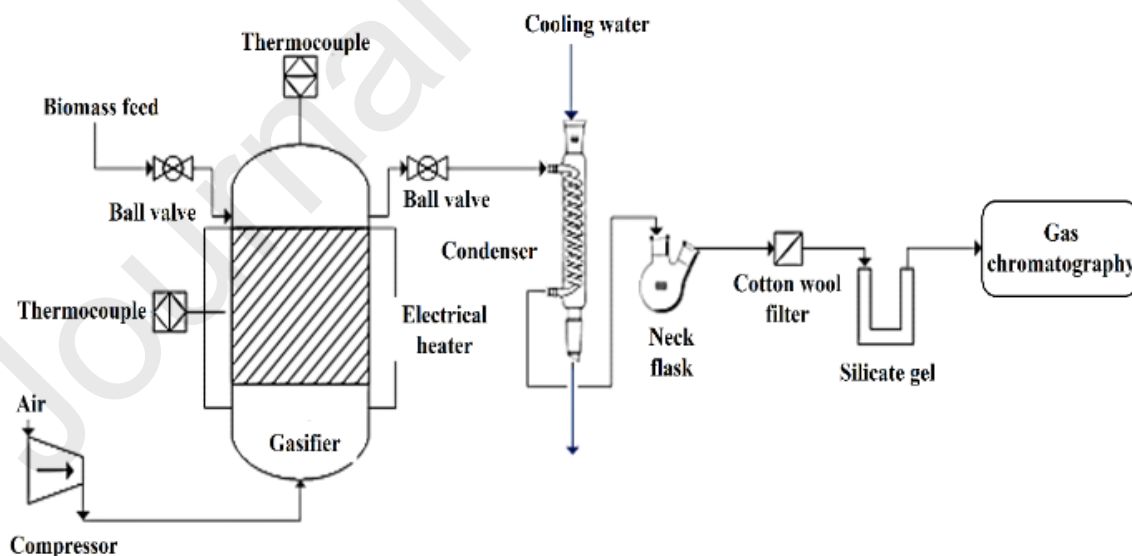

Fig. 1. Schematic diagram of lab scale updraft fluidised bed reactor.

6

The combustion tests of raw OPT, raw coal and coal-biocoal blends were performed in a fluidised bed reactor shown in **Fig. 1**. The minimum fluidisation velocity in the reactor, U_{mf} was determined by using Eq 1 [20] [21].

$$U_{mf} = \mu/D_\rho \rho_{air}[33.7^2 + 0.0408(D_\rho^3 \rho_{air}(\rho_p - \rho_{air})g)/\mu^2]^{\frac{1}{2}} - 33.7 \text{ (Eq 1)}$$

Where Re_{mf}, D_ρ, ρ_{air}, ρ_p, g, and μ represent the Reynolds number at minimum fluidisation velocity, diameter of sand particle (bed material), density of fluidising media (air), density of bed material, acceleration due to gravity and viscosity of fluid media, respectively.

Before start-up of the experiment, sand which was used as bed material was charged into the reactor at a depth-to-radius ratio of 1:1 [22]. The property of sand is presented in **Table 2**. Then the electric heater was switched on for 2 hours to heat up the reactor. Air was injected from air compressor into the reactor after the desired combustion temperature was achieved. 50 g of OPTC (100 wt%) was fed into the reactor when the bed temperature was in steady condition. The gas emitted from the reactor was collected in a 10.0 L Tedlar gas sampling bag and analysed using gas chromatography (Agilent Technology 6890N). At the end of each experiment, bio-liquid and ash produced from combustion of OPTC were collected and analysed. The combustion test was repeated for 50 g of sub-bituminous coal (SBC), raw OPT and blends of OPTC/SBC at biocoal to coal ratio of [0.2:1] (OPTC20) and [0.5:1](OPTC50) at the specified conditions for comparison study.

Table 2. Properties of bed material.

Bed materials	Geldart group	ρ (kg/m^3)	Particle size, dp (μm)
Sand	Group B (sand like) [23]	2650 [24, 25]	90 - 125

The combustion efficiency was determined using Eq 2.

E = [CO$_2$]/([CO$_2$] +[CO]) x 100 (Eq 2)

where [CO$_2$] and [CO] are the percentage of CO$_2$ and CO concentration in flue gas respectively.

2.3 Gas and ash analyses

Ash analysis was carried out using an energy dispersive x-ray fluorescence spectrometer (SHIMADZU EDX-720). Gas produced from the combustion process were analysed using gas chromatography (GC) (Agilent Technologies 6890N, Mundelein, IL, USA) equipped with a thermal conductivity detector (TCD).

2.4 Optimisation and statistical analyses

Response surface methodology (RSM) was conducted in Design-Expert 10 to study the effects of process temperature (A) and air flowrate (B) on concentration of CO2, [CO2] (v%) and combustion efficiency, E (%). The variable ranges are 600 °C – 900 °C for A and 10 – 20 standard cubic feet per hour (SCFH) (4.72 – 9.44 L/min) for B at fixed mass of the blended coal-biocoal. The flowchart of RSM algorithm is presented in **Fig. 2**. Analysis of variance was conducted to analyse the effect of air flowrate and combustion temperature on combustion efficiency and CO$_2$ production. **Table 3** summarises the proposed experimental conditions from the constructed model.

In RSM, it is assumed that the variables are quantitative and continuous. As discussed by Williges and Simon [26], central composite designs (CCD) is valuable in developing predictive models due to the following reasons. Firstly, the variance of an estimated response value is roughly undeviating over the experimental design region provided that suitable number of centre points is chosen. Therefore, experimental error can be estimated by replication at centre points. Secondly, to facilitate calculation, particular levels of the X variables are extended from the centre of the

design. Thirdly, the rotatability of numerous central composite designs entails dependency of predicted response reliability on distance of the point from the design centre and not direction.

Some of the limitations of RSM as discussed by Williges and Simon [26] are as follow. Firstly, there is a potential of increased prediction error if lower-order polynomials are used. Besides, the prediction beyond the region of the surface sampled should be avoided. The interpretation of the predictive equations should be conducted with care as the equations are convenient for making predictions and do not describe any fundamental or theory behind the observations.
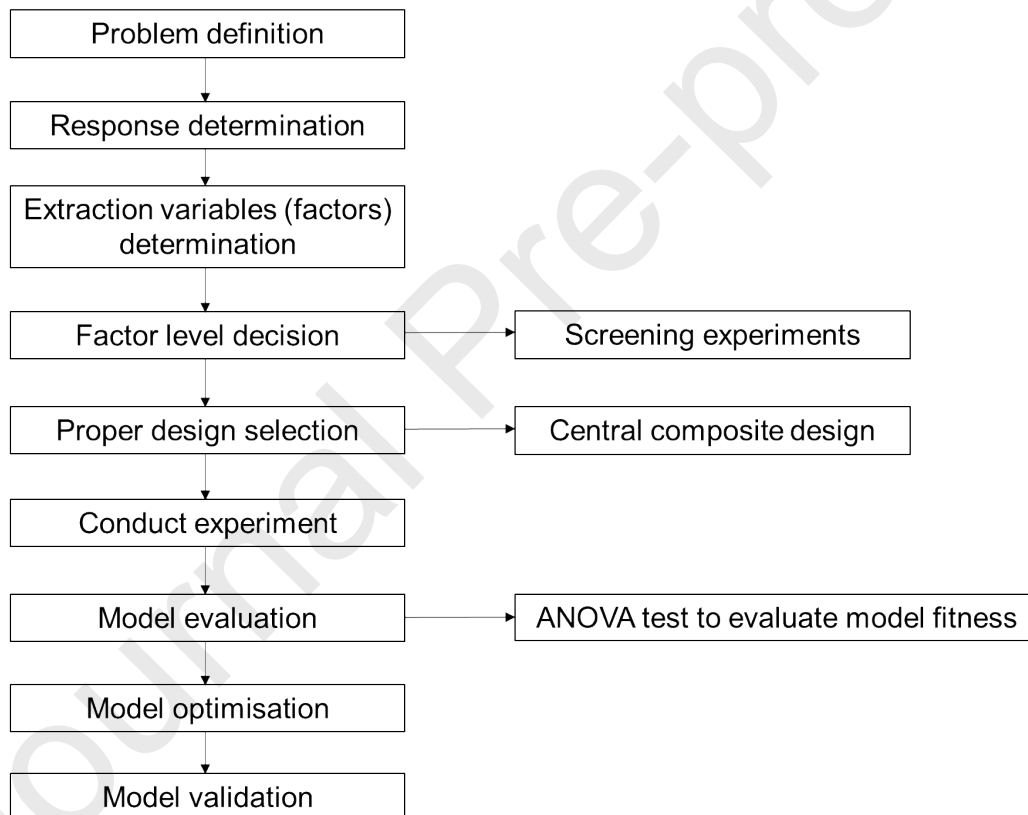
```
┌─────────────────────────┐
│    Problem definition    │
└─────────────────────────┘
            │
            ▼
┌─────────────────────────┐
│ Response determination   │
└─────────────────────────┘
            │
            ▼
┌─────────────────────────┐
│ Extraction variables (factors) │
│       determination       │
└─────────────────────────┘
            │
            ▼
┌─────────────────────────┐        ┌─────────────────────────┐
│  Factor level decision   │───────▶│  Screening experiments   │
└─────────────────────────┘        └─────────────────────────┘
            │
            ▼
┌─────────────────────────┐        ┌─────────────────────────┐
│ Proper design selection  │───────▶│ Central composite design │
└─────────────────────────┘        └─────────────────────────┘
            │
            ▼
┌─────────────────────────┐
│   Conduct experiment     │
└─────────────────────────┘
            │
            ▼
┌─────────────────────────┐        ┌──────────────────────────────────┐
│    Model evaluation      │───────▶│ ANOVA test to evaluate model fitness │
└─────────────────────────┘        └──────────────────────────────────┘
            │
            ▼
┌─────────────────────────┐
│   Model optimisation     │
└─────────────────────────┘
            │
            ▼
┌─────────────────────────┐
│    Model validation      │
└─────────────────────────┘
```

Fig. 2. Flowchart of RSM algorithm.

Table 3. Experimental runs constructed from RSM.

Run	Temperature (°C)	Air flowrate (SCFH)
1	650	12
2	650	12
3	650	12
4	850	12
5	850	12
6	850	12
7	650	18
8	650	18
9	650	18
10	850	18
11	850	18
12	850	18
13	600	15
14	600	15
15	900	15
16	900	15
17	750	10
18	750	10
19	750	20
20	750	20
21	750	15
22	750	15
23	750	15
24	750	15
25	750	15

3.0 Results and discussion

3.1 Combustion testing

CO_2 emission, combustion efficiency, NOx and SO_2 emission profiles from combustion of solid fuel blends at varying temperatures are presented in **Fig. 3, 4, 5 and 6** respectively.

Emission of CO_2 from combustion of fuel blends at varying temperatures is shown in **Fig. 3**. As shown in **Fig. 3**, coal emits the highest amount of CO_2 which is averaging around 18% throughout the temperature, followed by BIO20COAL80 which is 20% lesser and BIO50COAL50 at an average of 15%. The combustion of pure biocoal (OPTC) and biomass (OPTB) release much lower CO_2 concentration where the highest concentration of 7.7% was recorded at 767 °C for BIOCOAL100 while for BIOMASS100, the average concentration is lower by 35% compared to BIOCOAL100. The trend of CO_2 emission is in correlation with the carbon content within the fuel. This elucidates the highest and lowest CO_2 released by coal and biomass respectively, among the tested solid fuel blends [27]. The synergistic effect of CO_2 emission was observed in the blended fuels where the CO_2 concentration was higher for fuel blend with higher coal fraction. High temperature accelerates the progress of chemical reactions to form a high amount of carbon dioxide. However, as the temperature getting higher, rapid collision of the molecules leads to dissociation of molecules into atoms. Influenced by other factors such as particle size, turbulence and residence time, the atoms might disincline towards the formation of carbon dioxide but collide randomly to form other compounds such as carbon monoxide [28].
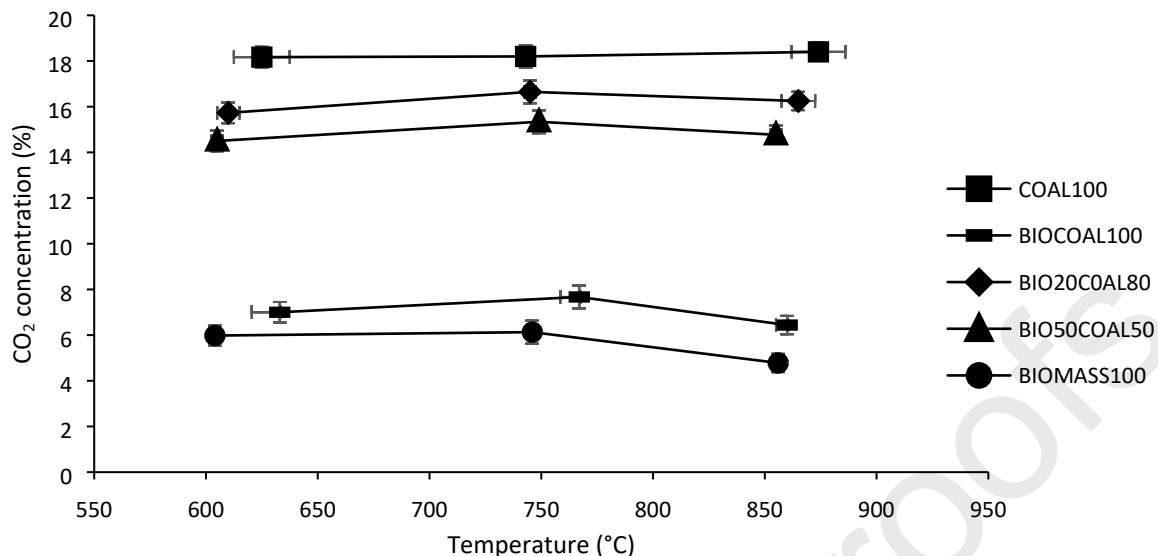
Fig. 3. CO_2 concentration from combustion of solid fuel blends at various temperatures.

The efficiency of the fuel blend combustion at varying temperature is presented in **Fig. 4**. As indicated in **Fig. 4**, the efficiency of pure biomass (BIOMASS100) and biocoal (BIOCOAL100) combustion records a significant increment as the temperature increases from 600 °C to 750 °C but diminishes at temperature beyond 800 °C. The highest efficiency recorded is 93.71% from combustion of pure biocoal (BIOCOAL100) at 767 °C, while the lowest efficiency recorded is 80.6% during combustion of pure biomass (BIOMASS100) at 600 °C. Fuel blends of 20% and 50% biocoal have average combustion efficiency within the range of 87% to 92%, suggesting that temperature has little effects on combustion of the blended fuels. This profile can be explained by the fact that as the temperature increases, dissociation tends to happen readily rendering the complete combustion become easier [29]. SBC has higher ignition temperature thus requires higher operating temperature (up to 900°C) for better combustion performance. Blending of OPTC into the coal improves the efficiency of SBC combustion since biomass and its derivative

12

compounds have high volatile matter. The synergistic effects can lower the ignition temperature and therefore enhance the efficiency of SBC combustion [30].
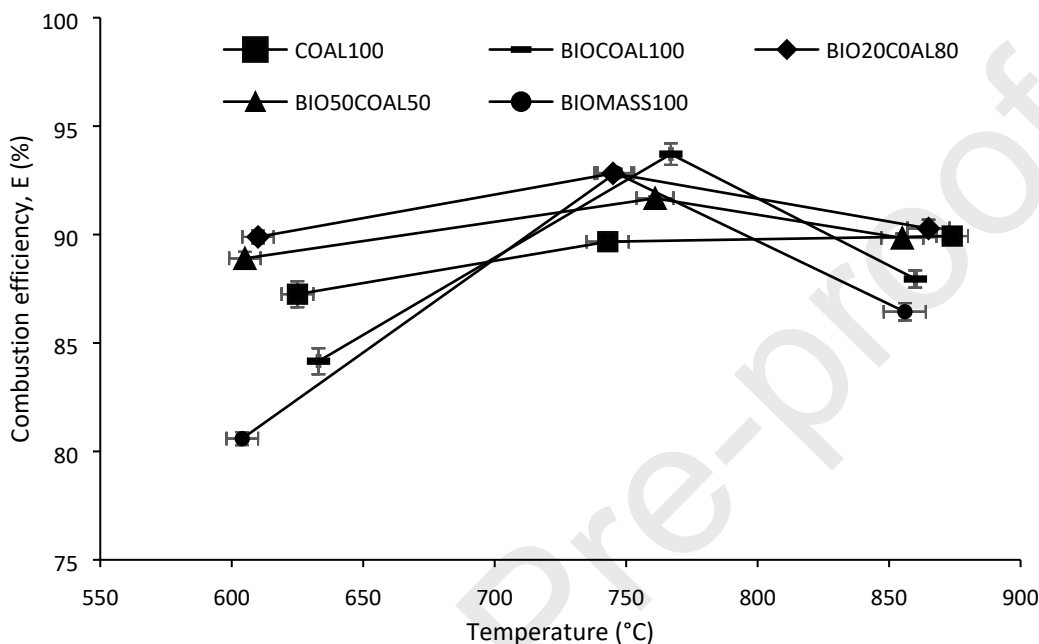

Fig. 4. Combustion efficiency of combustion of solid fuel blends at various temperatures.

As shown in **Fig. 5**, NOx emission profiles for all tested fuel blends are below the set limit of 296 ppm [31]. BIOCOAL100 has the highest emission at 250 ppm followed by BIO50COAL50, which is 12% lower and BIO20COAL80. All blended fuels and biomass (OPTB) exhibit higher NOx emissions compared to SBC. The findings are attributed to the nitrogen content within the fuels [32]. As the coal used in this study contains low amount of nitrogen, the amount of nitrogen compounds produced from the combustion process is low. On the other hand, biomass and biomass-derived fuels have slightly higher nitrogen content which consequently leads to higher emission of NOx [32]. The use of volatile matter as reburn fuel for NOx reduction is not possible since it has been removed during pyrolysis [33].
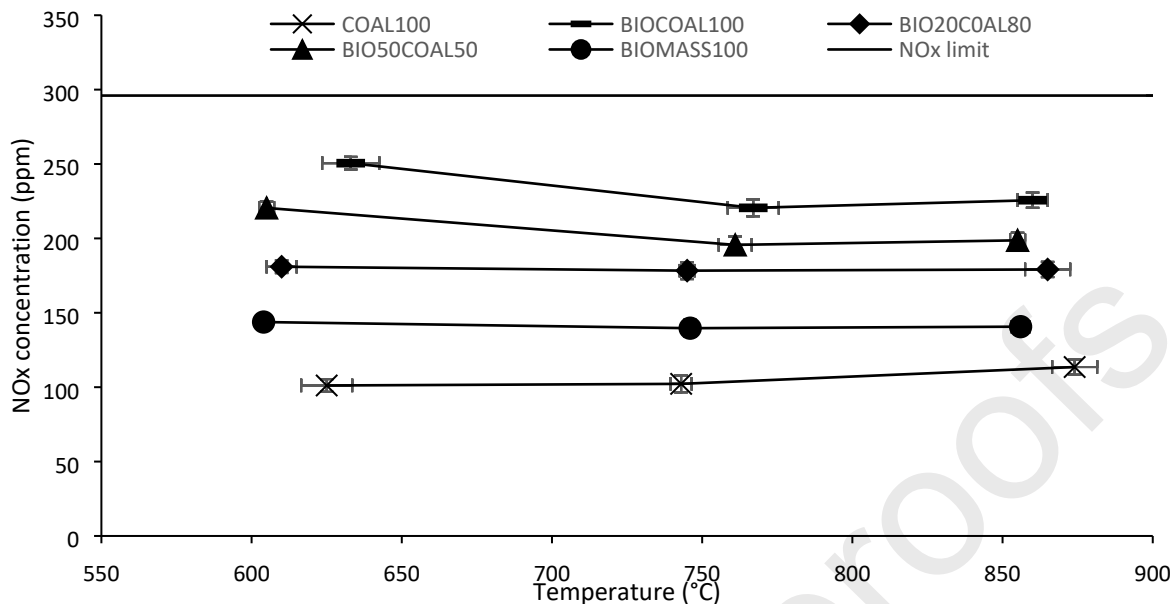
13

Fig. 5. NOx concentration profile from combustion of solid fuel blends at various temperatures.

Additionally, NOx concentration decreases as the temperature increases up to around 750 °C before slightly increase afterward for most samples except for coal. The highest NOx concentration of 250 ppm is recorded from combustion of BIOCOAL100 at 633 °C while the lowest NOx concentration of 101 ppm is recorded from combustion of 100 at 625 °C. The low NOx profiles correlate linearly with high combustion efficiency (see **Fig. 4**). The progression of combustion reactions towards completion will lead to high CO_2 production compared to other pollutants including NOx [34]. The combustion of SBC at higher temperatures is more efficient but generates a higher amount of NOx [35]. Reduction of NOx emission is possible by incorporating staged air combustion or flue gas recirculation into the combustion system. Staged air combustion adds primary air slightly below the stoichiometric ratio which promotes minimal emission of NOx, as well as ammonia and HCN from nitrogen content in the fuel [36]. Flue gas recirculation increases total mass flux of the gases while decreases the oxygen partial pressure and temperature within the gaseous mixture [37].

14

SO_2 emission profiles from combustion of the fuel blends are shown in **Fig. 6**. Among the five fuel blends, combustion of SBC produces the highest amount of SO_2 where the highest concentration is 62 ppm at combustion temperature of 874 °C. This is apparent as coal contains a higher amount of sulphur compared to other biomass-derived fuel blends. Blending of OPTC with SBC reduces SO_2 emission as sulphur is retained in biocoal ash in the form of solid alkali sulphates [33]. Similar to NOx emission profiles, the emission is considerably low which is far below the emission limit (190 ppm) imposed under Environmental Quality (Clean Air) Regulation 2014 [31].
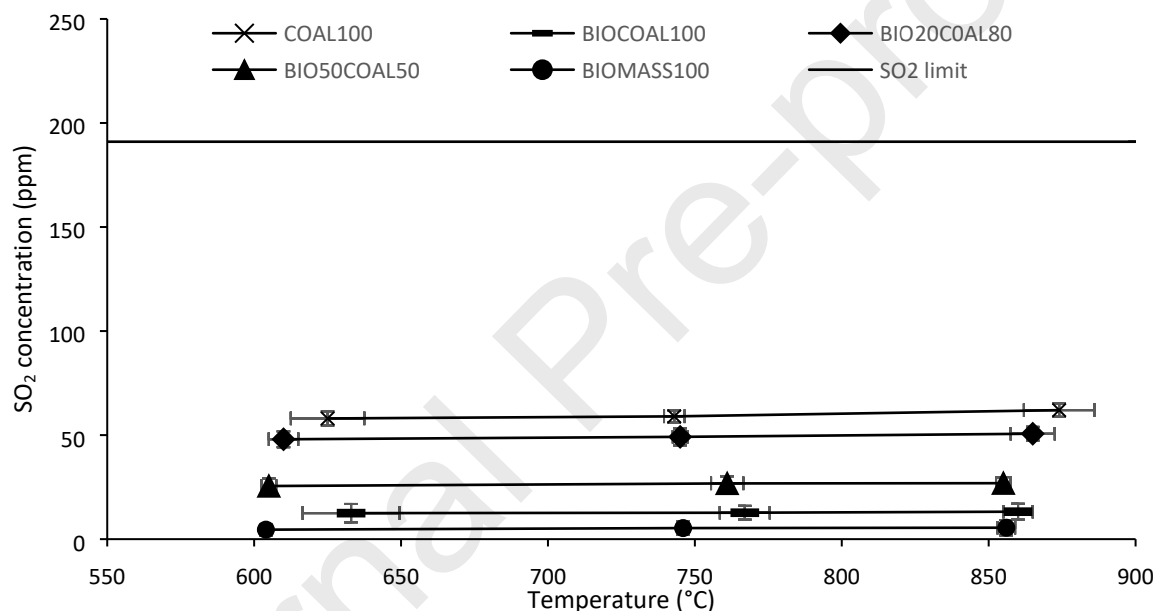

Fig. 6. SO_2 concentration profile from combustion of solid fuel blends at various temperatures.

According to statistics published by Energy Commission Malaysia, the total Malaysia energy supply in 2017 was 98,298 ktoe where coal and coke are the third biggest fuel type used with 21.1% share. Biomass, on the other hand, forms the third smallest portion in the supply with 0.2% share [38]. The potential benefits of co-firing or co-combustion of sub-bituminous coal / oil palm biomass fuel blends have been discussed in [12]. The discussion pertaining to improvement in

biofuel characteristics brought by pyrolysis of oil palm trunk biomass is available in [13]. In this study, oil palm trunk biomass (OPTB) is pyrolysed to produce oil palm trunk biocoal (OPTC) and subsequently co-combusted with sub-bituminous coal, which is currently used in Tenaga Nasional Berhad (TNB) Janamanjung power plant. The result shows that co-combustion of sub-bituminous coal with oil palm trunk biocoal improves combustion efficiency and emission of CO_2 and SO_2. While the proposed fuel blend might not be the best solution for conventional fuel replacement, improvement in combustion efficiency and emission of CO_2 and SO_2 should not be overlooked. Based on the positive impacts brought by blending of oil palm trunk derived biocoal with conventional low grade coal, the reliance on non-renewable coal for energy production can be reduced. Besides that, the biocoal can serve as a potential solid biofuel in the future. In addition, the problem of solid waste management in the oil palm plantation can be alleviated.

3.2 Optimisation study

Based on the findings from combustion testing, 20BIO80COAL is the best fuel blend for optimisation with RSM. The emission of CO_2, SO_2 and NOx from this formulation is reasonable with high combustion efficiency.

The experimental design and results are shown in **Table 4.** The results of ANOVA analysis that represents the effect and interaction of the operating parameters on the first response CO_2 concentration [CO2] are shown in **Table 5**.

Table 4. Experimental design with output responses based on the central composite design (CCD).

Run	Temperature, T (°C)	Air Flowrate (SCFH)	CO_2 concentration, $[CO_2]$ (%)	Combustion efficiency, E (%)
1	850	12	16.21	84.47
2	750	15	16.25	90.68
3	750	15	16.33	89.54
4	750	20	16.19	93.25
5	850	12	16.19	85.35
6	650	12	15.92	81.22
7	900	15	16.35	77.45
8	600	15	15.88	78.42
9	650	18	16.07	87.34
10	750	15	16.31	93.20
11	850	18	16.25	89.24
12	750	15	16.41	92.24
13	600	15	15.87	75.54
14	650	18	16.11	88.27
15	750	10	16.01	84.65
16	750	10	15.98	89.72
17	750	20	16.21	90.76
18	850	18	16.31	89.62
19	650	18	16.09	87.68
20	650	12	15.96	82.27
21	850	12	16.18	85.84
22	650	12	15.93	81.36
23	850	18	16.29	88.63
24	900	15	16.32	79.22
25	750	15	16.46	89.70

Table 5. ANOVA analysis for CO_2 concentration [CO2].

Source	Sum of squares	df	Mean square	F value	p-value Prob>F	
Model	0.67	5	0.13	56.34	< 0.0001	significant
A-Temperature	0.35	1	0.35	149.98	< 0.0001	
B-Air Flowrate	0.086	1	0.086	36.53	< 0.0001	
A^2	0.16	1	0.16	66.63	< 0.0001	
B^2	0.16	1	0.16	66.58	< 0.0001	
Residual	0.045	19	2.37E-03			
Lack of Fit	0.012	3	4.04E-03	1.97	0.1591	
Pure Error	0.033	16	2.05E-03			not significant
Cor Total	0.71	24				

The significance of the model is verified by a low P-value which is less than 0.0001 and high F-value of 56.34. P-value indicates the model significance while F-value depicts the influence of the operating parameters on the output responses [39, 40]. Based on statistical analyses conducted, temperature has a stronger influence on CO_2 emission compared to air flowrate. The empirical correlation that represents the interaction between CO_2 concentration with temperature and air flowrate is determined from second-order polynomial regression and shown in Eq 3.

$[CO_2] = 16.35 + 0.12A + 0.065B - 0.016AB - 0.11A^2$ (Eq 3)

The effects of the parameters and their interaction on CO_2 concentration are illustrated in the three-dimensional plot in **Fig. 7.**
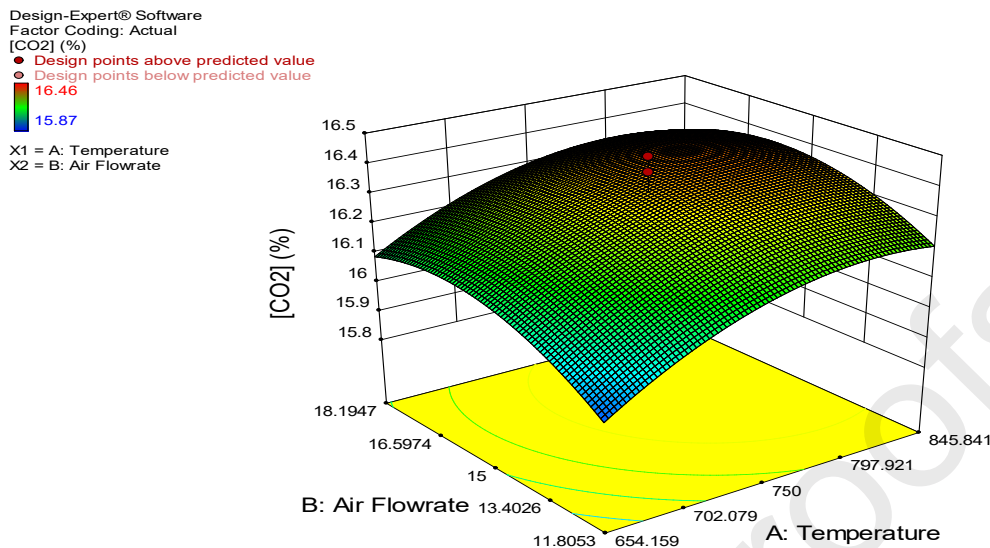
Fig. 7. The interaction between factors on CO_2 concentration.

As shown in **Fig. 7** and **Table 5**, temperature has a profound influence on CO_2 concentration with low P-value at less than 0.0001 and high F-value of 149.98. CO_2 concentration increases from 15.9% to 16.3% as the temperature increases from 600°C to 750°C. The dissociation of reactants at high temperature leads to the formation of gaseous products where CO_2 is the major constituent. In addition, high temperature promotes the free energy within the system to overcome the minimal activation energy needed for CO_2 formation. This finding is in agreement with a kinetic study on biochar combustion where CO and CO_2 formation is favoured at elevated temperature [41].

Air flowrate has lower influence on CO_2 concentration compared to reaction temperature with F-value of 36.53 and low P-value of 0.0001. CO_2 concentration increases from 15.92% to 16.11% when the air flowrate is increased from 12 SCFH (5.66 litre per minute) to 18 SCFH (8.5 litre per minute). The increment is higher when air flowrate is combined with temperature, which is a dominant variable in this study. Air injection into the combustion system within the predefined time creates turbulence which promotes random swirl motion that aids even distribution of fuel

19

particles. The phenomenon accelerates heat transfer within fuel particles and thus assisting devolatilisation and the subsequent reactions [42]. The CO_2 production will be retarded at very high temperature and air flowrate. This pattern is consistent with findings in [43].

The ANOVA analysis for combustion efficiency, E is shown in **Table 6.**

Table 6. The ANOVA analysis for combustion efficiency.

Source	Sum of squares	df	Mean square	F value	p-value Prob > F	
Model	560.58	5	112.12	38.59	< 0.0001	significant
A-Temperature	17.31	1	17.31	5.96	0.0246	
B-Air Flowrate	92.86	1	92.86	31.96	< 0.0001	
A^2	392.98	1	392.98	135.26	< 0.0001	
B^2	2.66	1	2.66	0.92	0.3507	
Residual	55.20	19	2.91			
Lack of Fit	20.69	3	6.90	3.20	0.0518	not significant
Pure Error	34.52	16	2.16			
Cor Total	615.78	24				

A Low P-value of 0.0001 and a high F-value of 38.59 validate the significance of the model for the prediction of combustion efficiency. Based on the P and F values, the influence of variables on combustion efficiency can be observed. In comparison to CO_2 generation, the effect of air flowrate on combustion efficiency is more dominant than temperature. From regression analysis, the mathematical equation to calculate the combustion efficiency of the process is presented in Eq 4.

E1= 91.38 + 0.87A + 2.13B - 0.56AB - 5.24A^2 - 0.44B^2 (Eq 4)

The combined effects of air flowrate and process temperature on combustion efficiency are graphically presented in **Fig. 8**. The plot shows that at a temperature of 750 °C, combustion

efficiency increases as air flowrate increases up to 18.2 SCFH (8.59 litre per minute) to reach maximum efficiency of 93%. The combustion process becomes less efficient after further increment in temperature beyond 750 °C at air flowrate of 18.2 SCFH. The efficiency of the combustion process is low at low air flowrate and further increment in temperature beyond 750 °C will reduce the efficiency even lower. The same trend was observed by Suranani and Goli [44]. Excess air from high air flowrate enhances the combustion efficiency as more oxygen is being supplied into the system [45].
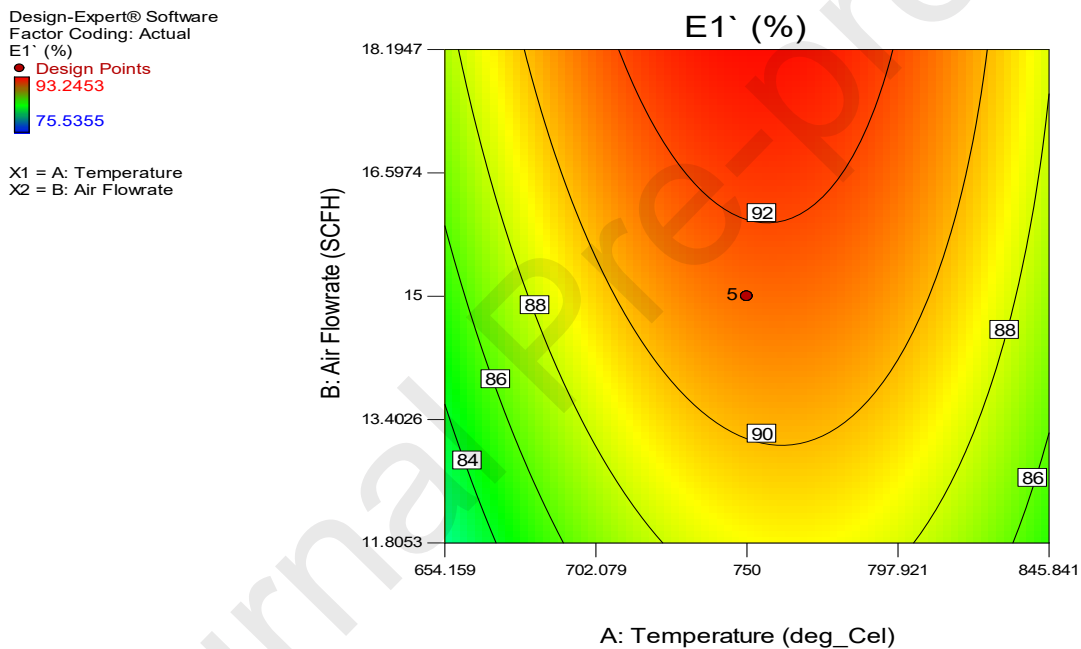
Fig. 8. The contour plot of the variable combined effects on combustion efficiency.

Based on statistical analyses, the optimised conditions for combustion of oil palm trunk biocoal are achieved at temperature of 774 °C and air flowrate of 16.6 SCFH with a desirability value of 0.896. The predicted CO_2 concentration and combustion efficiency at optimum conditions are

16.38% and 92.2% respectively. The simulated conditions and outcomes are validated against experimental works and the findings are summarised in **Table 7**. The predicted values demonstrate an acceptable agreement with the experimental results. The standard deviation for CO_2 concentration and combustion efficiency is 0.11 and 0.29 respectively.

Table 7. Comparison between predicted and experimentally measured CO_2 concentration and combustion efficiency at optimised conditions.

	Factors		Responses	
	Temperature (°C)	Air flowrate (SCFH)	[CO2](%)	E1 (%)
Predicted values	774	16.6	16.38	92.16
Experiment 1	779	16.5	17.15	92.70
Experiment 2	770	16.8	15.73	90.38
Experiment 3	773	16.5	16.88	91.74
Average	774	16.6	16.53	91.74
Standard deviation	-	-	0.11	0.29

3.3 Ash analysis

Fig. 9 shows the XRD pattern of the ash sample from the optimised combustion run. Broad diffraction background and several sharp peaks are observed, suggesting equally crystalline and amorphous structure. Broad peaks are observed in the lower 2θ region (25°) and at 67° in the spectrum. The degree of crystallinity as calculated by Match 3 software is 44.59%. The remaining components of biocoal which are mostly lignin are attributed to the amorphous phase due to the lack of larger crystal formation. The constituents of crystalline phases present in the ash are shown in **Table 8.**
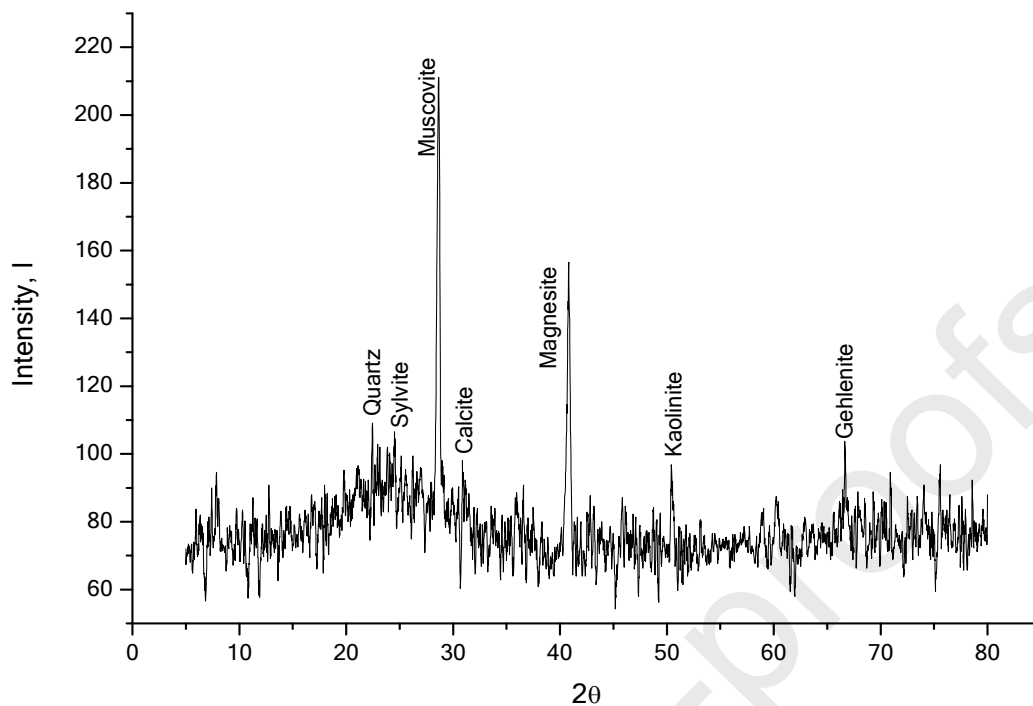
Fig. 9. The XRD pattern of coal-biocoal blend.

Table 8. Fraction of crystalline phases in ash.

Phases	Quantity (%)
Muscovite	29.2
Kaolinite	19.3
Gehlenite	10.2
Quartz	9.2
Calcite	7.6
Magnesite	5.9
Sylvite	5.7
Pyrite	4.0
Dolomite	3.3
Hematite	2.9
Portlandite	2.7

Table 8 shows that major components in the ash are silicone, Si-containing compounds (muscovite, kaolinite, gehlenite and quartz). This is expected as Si is abundant in minerals such as coal in the form of silicon dioxide. Small fractions of dolomite, hematite and portlandite are present

23

below 4%. Thus, it is expected that the slagging propensity of the coal-biocoal blend is much lower due to the abundance of Si oxides in the ash. Moreover, as the blending ratio is dominated by sub-bituminous coal particles (20% biocoal), compounds with high melting points are likely to form during combustion [46]. Basic metal oxides are found within 100% biocoal which result in the formation of compounds with low melting point that has high slagging tendency. Therefore, blending coal with OPT biocoal has the potential to reduce slagging possibility. Fouling tendency, on the other hand, is expected to be significant even with the presence of high amount of Si oxides which are abundant in coal.

Besides, calcite was detected in the ash sample. This compound decomposes at 700 – 900 °C into CO_2 and calcium oxide (CaO). Subsequently, CaO reacts with silica and other compounds to form silicates, which are abundant in the ash sample. Febrero, Granada *et al.* [47] concluded that the presence of calcite indicates that the high temperature was not uniformly reached within the combustion burner. This phenomenon however depends on other factors such as fuel size and particle size distribution. The heating of calcite at low or medium temperature leads to the formation of portlandite [48]. Gehlenite, which is the third abundant mineral phase found in the ash is formed from carbonate-silicate-spinel reactions. According to Koukouzas, Hämäläinen *et al.* [49], based on their studies, gehlenite is formed from silicon dioxide and calcium within coal-wood chips fuel blend. The presence of 5.7% sylvite in the ash is due to the high alkali content in the biomass [49].

4.0 Conclusions

In this study, particles of OPTB was pyrolysed in a top lift updraft, autothermal-heated furnace to produce OPTC. The biocoal was blended with SBC at various coal-to-biocoal ratio and subsequently co-fired in a combustion unit. The result shows that co-combustion of sub-bituminous coal with oil palm trunk biocoal improves combustion efficiency and emission of CO_2 and SO_2. While the proposed fuel blend might not be the best solution for conventional fuel replacement, improvement in combustion efficiency and emission of CO_2 and SO_2 should not be overlooked. Based on the positive impacts brought by blending of oil palm trunk derived biocoal with conventional low-grade coal, the reliance on non-renewable coal for energy production can be reduced. Besides that, the biocoal can serve as a potential solid biofuel in the future. In addition, the problem of solid waste management in the oil palm plantation can be alleviated. The blending of novel oil palm trunk biocoal with conventional low-grade coal brings a positive impact to the area of energy conversion and management

List of abbreviations

ANOVA   Analysis of variance

CCD   Central composite design

GHG   Greenhouse gases

OPF   Oil palm frond

OPT   Oil palm trunk

OPTB   Oil palm trunk biomass

OPTC   Oil palm trunk biocoal

RSM   Response surface methodology

SBC   Sub-bituminous coal

SCFH   Standard cubic feet hour

TNB   Tenaga Nasional Berhad

XRD   X-ray diffraction

Funding

Declaration of competing Interest

The authors declare no conflict of interests.

Acknowledgments

References

[1] Y.-F. Huang, P.-T. Chiueh, S.-L. Lo. A review on microwave pyrolysis of lignocellulosic biomass. Sustainable Environment Research. 26 (2016) 103-9. https://doi.org/10.1016/j.serj.2016.04.012.

[2] M.S. Md Said, W.A. Wan Abdul Karim Ghani, T. Hong Boon, S.A. Hussain, D.K.S. Ng. Thermochemical Conversion of Napier Grass for Production of Renewable Syngas. Processes. 7 (2019) 705. https://doi.org/10.3390/pr7100705.

[3] Y.-F. Huang, P.-H. Cheng, P.-T. Chiueh, S.-L. Lo. Leucaena biochar produced by microwave torrefaction: Fuel properties and energy efficiency. Applied Energy. 204 (2017) 1018-25. https://doi.org/10.1016/j.apenergy.2017.03.007.

[4] Y. Qi, N. Stern, J.-K. He, J.-Q. Lu, T.-L. Liu, D. King, et al. The policy-driven peak and reduction of China's carbon emissions. Advances in Climate Change Research. 11 (2020) 65-71. https://doi.org/10.1016/j.accre.2020.05.008.

[5] Energy Commission. MALAYSIA ENERGY STATISTICS HANDBOOK 2018. 2019.

[6] M.A. Sukiran, F. Abnisa, W.M.A. Wan Daud, N. Abu Bakar, S.K. Loh. A review of torrefaction of oil palm solid wastes for biofuel production. Energy Conversion and Management. 149 (2017) 101-20. https://doi.org/10.1016/j.enconman.2017.07.011.

[7] S.K. Loh. The potential of the Malaysian oil palm biomass as a renewable energy source. Energy Conversion and Management. 141 (2017) 285-98. https://doi.org/10.1016/j.enconman.2016.08.081.

[8] S. Surip, M. Jawaid, A.K. H.P.S, A. Mohamed, F. Ibrahim. A review of oil palm biocomposites for furniture design and applications: Potential and challenges. Bioresources. 7 (2012) 4400-23.

[9] I.-Y. Eom, J.-H. Yu, C.-D. Jung, K.-S. Hong. Efficient ethanol production from dried oil palm trunk treated by hydrothermolysis and subsequent enzymatic hydrolysis. Biotechnology for Biofuels. 8 (2015) 83. 10.1186/s13068-015-0263-6.

[10] P. Shrivastava, P. Khongphakdi, A. Palamanit, A. Kumar, P. Tekasakul. Investigation of physicochemical properties of oil palm biomass for evaluating potential of biofuels production via pyrolysis processes. Biomass Conversion and Biorefinery. (2020). 10.1007/s13399-019-00596-x.

[11] A.K. Tareen, I.N. Sultan, K. Songprom, N. Laemsak, S. Sirisansaneeyakul, W. Vanichsriratana, et al. Two-step pretreatment of oil palm trunk for ethanol production by thermotolerent Saccharomyces cerevisiae SC90. Bioresource Technology. 320 (2021) 124298. https://doi.org/10.1016/j.biortech.2020.124298.

[12] S.S. Idris, N.A. Rahman, K. Ismail. Combustion characteristics of Malaysian oil palm biomass, sub-bituminous coal and their respective blends via thermogravimetric analysis (TGA). Bioresource Technology. 123 (2012) 581-91. https://doi.org/10.1016/j.biortech.2012.07.065.

[13] N.A. Nudri, R.T. Bachmann, W.A.W.A.K. Ghani, D.N.K. Sum, A.A. Azni. Characterization of oil palm trunk biocoal and its suitability for solid fuel applications. Biomass Conversion and Biorefinery. 10 (2020) 45-55. 10.1007/s13399-019-00419-z.

[14] P. Sakulkit, A. Palamanit, R. Dejchanchaiwong, P. Reubroycharoen. Characteristics of pyrolysis products from pyrolysis and co-pyrolysis of rubber wood and oil palm trunk biomass for biofuel and value-added applications. Journal of Environmental Chemical Engineering. 8 (2020) 104561. https://doi.org/10.1016/j.jece.2020.104561.

[15] N.S. Kamal Baharin, V.C. Koesoemadinata, S. Nakamura, W.J. Yahya, M.A. Muhammad Yuzir, F.N. Md Akhir, et al. Conversion and characterization of Bio-Coke from abundant biomass waste in Malaysia. Renewable Energy. 162 (2020) 1017-25. https://doi.org/10.1016/j.renene.2020.08.083.

[16] H.K. Nsamba, S.E. Hale, G. Cornelissen, R.T. Bachmann. Improved Gasification of Rice Husks for Optimized Biochar Production in a Top Lit Updraft Gasifier. Journal of Sustainable Bioenergy Systems. 4 (2014) 225-42. http://dx.doi.org/10.4236/jsbs.2014.44021.

[17] R.R.R. Deris, M.R. Sulaiman, F.M. Darus, M.S. Mahmud, N.A. Bakar. Pyrolysis of oil palm trunk (OPT). 20th Symp Malayisan Chem Eng (SOMChE) 20062006. pp. 245-50.

[18] Phyllis2. coal, lignite (#2847).

[19] P. Costen, F.C. Lockwood, J.J. Ou. Analysis of solid waste fuels, APAS Clean Coal Technology. London (UK), Imperial College of Science, Technology and Medicine.

[20] M.S.M. Said, W.A.W.A.K. Ghani, T.H. Boon, D.N.K. Sum. Prediction and Optimisation of Syngas Production from Air Gasification of Napier Grass via Stoichiometric Equilibrium Model.

28

Energy Conversion and Management: X. (2020) 100057. https://doi.org/10.1016/j.ecmx.2020.100057.

[21] C. Wen, Y. Yu. A generalized method for predicting the minimum fluidization velocity. AIChE Journal. 12 (1966) 610-2.

[22] Y. Cao, Y. Wang, J.T. Riley, W.-P. Pan. A novel biomass air gasification process for producing tar-free higher heating value fuel gas. Fuel Processing Technology. 87 (2006) 343-53. https://doi.org/10.1016/j.fuproc.2005.10.003.

[23] D. Geldart. Types of gas fluidization. Powder Technology. 7 (1973) 285-92. https://doi.org/10.1016/0032-5910(73)80037-3.

[24] F. Fotovat, R. Ansart, M. Hemati, O. Simonin, J. Chaouki. Sand-assisted fluidization of large cylindrical and spherical biomass particles: Experiments and simulation. Chemical Engineering Science. 126 (2015) 543-59. https://doi.org/10.1016/j.ces.2014.12.022.

[25] A.M. Sharma, A. Kumar, K.N. Patil, R.L. Huhnke. Fluidization characteristics of a mixture of gasifier solid residues, switchgrass and inert material. Powder Technology. 235 (2013) 661-8. https://doi.org/10.1016/j.powtec.2012.11.025.

[26] R.C. Williges, C.W. Simon. Applying Response Surface Methodology to Problems of Target Acquisition. Human Factors. 13 (1971) 511-9. 10.1177/001872087101300602.

[27] T. Kühn, J.R. Bunt, H.W.J.P. Neomagus, S.J. Piketh, R.C. Everson, S. Coetzee. Coal-derived low smoke fuel assessment through coal stove combustion testing. Journal of Analytical and Applied Pyrolysis. 126 (2017) 158-68. https://doi.org/10.1016/j.jaap.2017.06.012.

[28] A. Williams, J.M. Jones, L. Ma, M. Pourkashanian. Pollutants from the combustion of solid biomass fuels. Progress in Energy and Combustion Science. 38 (2012) 113-37. https://doi.org/10.1016/j.pecs.2011.10.001.

[29] R.A. Strehlow. Combustion Fundamentals. McGraw-Hill1984.

[30] J. Riaza, J. Gibbins, H. Chalmers. Ignition and combustion of single particles of coal and biomass. Fuel. 202 (2017) 650-5. https://doi.org/10.1016/j.fuel.2017.04.011.

[31] M. Motokura, J. Lee, I. Kutani, H. Phoumin. Improving Emissions Regulation for Coal-fired Power Plants in ASEAN. ERIA Research Project Report2017.

[32] S.G. Sahu, N. Chakraborty, P. Sarkar. Coal–biomass co-combustion: An overview. Renewable and Sustainable Energy Reviews. 39 (2014) 575-86. https://doi.org/10.1016/j.rser.2014.07.106.

[33] A. Demirbaş. Sustainable cofiring of biomass with coal. Energy Conversion and Management. 44 (2003) 1465-79. https://doi.org/10.1016/S0196-8904(02)00144-9.

[34] W.A.W.A.K. Ghani, R.A. Moghadam, M.A.M. Salleh. Air Gasification of Malaysia Agricultural Waste in a Fluidized Bed Gasifier: Hydrogen Production Performance Sustainable Growth and Applications in Renewable Energy Sources2011.

[35] J. Hou, Y. Ma, S. Li, W. Shang. A comparative study on characteristics of sulfur and nitrogen transformation and gaseous emission for combustion of bituminous coal and char. Carbon Resources Conversion. 1 (2018) 86-93. https://doi.org/10.1016/j.crcon.2018.04.004.

[36] J. Wang, W. Fan, Y. Li, M. Xiao, K. Wang, P. Ren. The effect of air staged combustion on NOx emissions in dried lignite combustion. Energy. 37 (2012) 725-36. https://doi.org/10.1016/j.energy.2011.10.007.

[37] R. Bauer, M. Gölles, T. Brunner, N. Dourdoumas, I. Obernberger. Modelling of grate combustion in a medium scale biomass furnace for control purposes. Biomass and Bioenergy. 34 (2010) 417-27. https://doi.org/10.1016/j.biombioe.2009.12.005.

[38] Energy Commission Malaysia. Malaysia Energy Statistics Handbook 2019. 2020.

[39] M. Shahbaz, S. Yusup, A. Inayat, D.O. Patrick, A. Pratama. Application of response surface methodology to investigate the effect of different variables on conversion of palm kernel shell in steam gasification using coal bottom ash. Applied Energy. 184 (2016) 1306-15. https://doi.org/10.1016/j.apenergy.2016.05.045.

[40] A.R. Mohamad Daud. Energy densified biochar production from slow pyrolysis of reed canary grass. 10 (2015) 7196-201.

[41] M. Morin, S. Pécate, M. Hémati. Kinetic study of biomass char combustion in a low temperature fluidized bed reactor. Chemical Engineering Journal. 331 (2018) 265-77. https://doi.org/10.1016/j.cej.2017.08.063.

[42] M. Gu, M. Zhang, W. Fan, L. Wang, F. Tian. The effect of the mixing characters of primary and secondary air on NOx formation in a swirling pulverized coal flame. Fuel. 84 (2005) 2093-101. https://doi.org/10.1016/j.fuel.2005.04.019.

[43] Y.B. Yang, V.N. Sharifi, J. Swithenbank. Effect of air flow rate and fuel moisture on the burning behaviours of biomass and simulated municipal solid wastes in packed beds. Fuel. 83 (2004) 1553-62. https://doi.org/10.1016/j.fuel.2004.01.016.

[44] S. Suranani, V.R. Goli. Fuel Particle Size Effect on Performance of Fluidized Bed Combustor Firing Ground Nutshells. International Journal of Chemical Engineering and Applications. 3 (2012) 147-51. 10.7763/IJCEA.2012.V3.176.

[45] T. Madhiyanon, P. Sathitruangsak, S. Soponronnarit. Co-combustion of rice husk with coal in a cyclonic fluidized-bed combustor (ψ-FBC). Fuel. 88 (2009) 132-8. https://doi.org/10.1016/j.fuel.2008.08.008.

[46] S.-X. Zhao, N. Ta, X.-D. Wang. Effect of Temperature on the Structural and Physicochemical Properties of Biochar with Apple Tree Branches as Feedstock Material. Energies. 10 (2017) 1293.

[47] L. Febrero, E. Granada, A. Regueiro, J.L. Míguez. Influence of Combustion Parameters on Fouling Composition after Wood Pellet Burning in a Lab-Scale Low-Power Boiler. Energies. 8 (2015) 9794-816.

[48] A. Filippidis, A. Georgakopoulos. Mineralogical and chemical investigation of fly ash from the Main and Northern lignite fields in Ptolemais, Greece. Fuel. 71 (1992) 373-6. https://doi.org/10.1016/0016-2361(92)90024-I.

[49] N. Koukouzas, J. Hämäläinen, D. Papanikolaou, A. Tourunen, T. Jäntti. Mineralogical and elemental composition of fly ash from pilot scale fluidised bed combustion of lignite, bituminous coal, wood chips and their blends. Fuel. 86 (2007) 2186-93. https://doi.org/10.1016/j.fuel.2007.03.036.